

Effect of the base pressure achieved prior deposition on the main properties of ZnO:Al (AZO) films obtained by DC magnetron sputtering at room temperature for electrical contact use

J.A. García-Valenzuela,^{a)} J. Andreu, and J. Bertomeu

Departament de Física Aplicada (FA), Universitat de Barcelona (UB), Carrer de Martí i Franquès 1–11, C.P. 08028, Barcelona, Catalonia, Spain.

^{a)} Electronic mail: jgarciavlz@gmail.com, jgarciavlz@ub.edu

The effect that the base pressure achieved prior to deposition has upon the electrical, optical, structural, and chemical properties of ZnO:Al (aluminum-zinc oxide, AZO) thin films was studied. The thin films were obtained at room temperature on glass substrates by direct-current (DC) magnetron sputtering with a power of 120 W (corresponding to a power density of 2.63 W/cm^2) and a total deposition pressure of 4.0 mTorr (0.53 Pa) with only argon gas. It was observed that all AZO characteristics and properties varied with base pressure without following a simple tendency, although some correlation was found between the crystallinity and deposition rate, with the latter depending directly upon the achieved base pressure. However, three distinct vacuum zones were identified, each of which produced AZO thin films that exhibited similar characteristics and properties. Among the base pressures studied, the lower base pressure zone [best vacuum level: under $\sim 5.7 \times 10^{-7}$ Torr ($\sim 7.6 \times 10^{-5}$ Pa); dark yellow zone] produced dark yellow AZO thin films with moderate transmittance, but the highest resistivity and the worst stability to the environment. The middle base pressure zone [$\sim 5.7 \times 10^{-7}$ Torr ($\sim 7.6 \times 10^{-5}$ Pa) to $\sim 7.3 \times 10^{-7}$

⁷ Torr ($\sim 9.7 \times 10^{-5}$ Pa); opaque zone] produced dark gray or brown AZO thin films with good conductivity, but that exhibited the worst transmittance. The higher base pressure zone [bad vacuum level: higher than $\sim 7.3 \times 10^{-7}$ Torr ($\sim 9.7 \times 10^{-5}$ Pa); transparent zone] produced highly transparent AZO thin films with moderate resistivity. The best AZO thin film was deposited after achieving this transparent base pressure zone, but specifically in the transparent–opaque border [$\sim 7.35 \times 10^{-7}$ Torr ($\sim 9.80 \times 10^{-5}$ Pa)]. It was found that the films deposited near this transparent–opaque border within a wide margin in the direction of the transparent zone (to higher base pressure) exhibited the best transmittance, conductivity, and stability to the environment. The use of this moderate vacuum level is therefore recommended for the deposition of AZO thin films.

Keywords:

Al-doped zinc oxide, transparent conductive oxide, sputtering, base pressure, vacuum.

I. INTRODUCTION

Magnetron sputtering is a technique that currently dominates the industry of metallic and metal oxide film deposition. Similarly, at the laboratory scale, magnetron sputtering is the deposition technique of choice. Because this is a vacuum technique, researchers typically desire systems that achieve the best vacuum levels, which is a requirement that is justified in the “conventional” fact that residual gases (from air) are incorporated as contaminants and can deteriorate the properties of the sputtering-deposited films. With this in mind, companies involved in sputtering equipment production have included pumping systems achieving even ultra-high vacuum (UHV) levels ($<10^{-9}$ Torr), which have become very popular both in industry and in research laboratories.

However, it is not obvious that the UHV regime is essential for sputtering deposition. It is most likely that the need for UHV depends on the kind of material to be deposited and how the residual gases can affect them. This raises the even more important question of which vacuum levels are acceptable for the sputtering deposition of most common materials. Fortunately, some publications related to this subject exist, where the authors address the real effect of different levels of residual gases on the properties of a given deposited material.

Most of these studies focused on the effect of controlled quantities of a specific known ambient gas—water vapor, H_2 , N_2 , or O_2 —on specific properties of the material in which they were interested. Although the study of the effect of controlled ambient gasses provides valuable information, the base pressure achieved prior to sputtering deposition of a given material must also be studied, since this constitutes a real deposition variable that, unfortunately, is sometimes not taken into account.

In these studies, the first interest of the effect of base pressure was on the properties of metallic films, specifically in the deposition of Al-Si alloys,¹ Co/Cu multilayers,² Mo/Si multilayers,^{3,4} Fe-Pt alloys,^{5,6} Sm-Fe alloys,⁷ Mo,⁸ and Al thin films.⁹ In these works the authors generally concluded that a high base pressure (low vacuum) is detrimental to the desired properties of the deposited films, and especially in the reflectivity. Therefore, they recommended a maximum evacuation of residual ambient gases. Similar results were observed in the properties expected for AgInSbTe¹⁰ and B₄C,¹¹ but the change in base pressure did not seem to greatly affect the desired properties of nitrides such TiN_xO_y¹² and AlN.¹³

On the other hand, the study of the effect of base pressure on the properties of metal oxides deposited from ceramic targets such as Sn-doped In₂O₃ (In₂O₃:Sn), known as indium-tin oxide (ITO),^{14,15} and its better substitute as transparent conductive oxide (TCO), Al-doped ZnO (ZnO:Al), known as aluminum-zinc oxide (AZO),¹⁶⁻¹⁸ produced interesting results. In these cases, the authors presented different outcomes regarding the effect of the base pressure on the optical and electrical properties of the deposited films, because most of the properties were studied as a function of three or four points of base pressure. The most complete work was that reported by Zebaze-Kana *et al.*,¹⁵ who tested a moderate range of the base pressure and observed that the increase of this parameter, up to a certain value, leads to a decrease of ITO resistivity, which then increases with a further increase of base pressure. This behavior of the resistivity will be referred to in this work as the U-shaped tendency. Furthermore, it is also important to note that Zebaze-Kana *et al.*¹⁵ observed that the transmittance of ITO, on the other hand, always increased with the increase of the base pressure.

To understand the above observations regarding the electrical and optical properties of ITO and AZO thin films, it is necessary to consider the results reported about the effect of controlled quantities of ambient gases on such properties, which is actually an issue widely studied. Curiously, the effect of the partial pressure of water vapor^{19,20} or H₂²¹⁻²⁹ on the resistivity of ITO films exhibits the same U-shaped behavior reported by Zebaze-Kana *et al.*¹⁵ concerning the effect of base pressure. The same U-shaped tendency was observed in the resistivity of AZO films with the addition of H₂ in the sputtering chamber.³⁰⁻³⁶ Although we failed to find any systematic study of the effect of water vapor on the properties of AZO, we suppose the same U-shaped behavior exists there as well. Therefore, because water vapor is the main residual ambient gas present when evacuating a sputtering chamber,^{3,14} and because water vapor produces hydrogen atoms in the plasma discharge, we can then associate the previously mentioned effect of water vapor and H₂ with the effect of base pressure reported by Zebaze-Kana *et al.*¹⁵ on ITO properties. Thus, we can conclude the importance of testing a wide range of base pressures to form a solid conclusion about its effect on the properties of a given material and, more importantly, to identify the maximum base pressure that can be tolerated.

For the case of TCOs, which are materials of particular interest, we can consider that the different properties reported in the literature for the same material under the same typical deposition parameters can be related also to the different base pressure values used in those works. Although we demonstrate in this paper, for the AZO case in particular, that there is a wide range of base pressures in which the properties of the deposited material are almost constant, there is also a narrow base pressure range in which the measured properties are the best. Furthermore, we demonstrate that, by

improving the vacuum level beyond this narrow interval, all of the properties change enormously. For this, we tested a wide range of values to observe the effect of base pressure achieved prior to deposition on the electrical, optical, structural, and chemical properties of AZO thin films deposited on glass substrates by direct-current (DC) magnetron sputtering at room temperature.

II. EXPERIMENTAL

A. Deposition methodology

The deposition equipment used herein was a commercial ATC-ORION 8 HV sputtering system from AJA International, Inc. It consisted of a 34.7-cm diameter and 39.8-cm height chamber with 3 different magnetron guns in a con-focal geometry. In this configuration, the magnetron sputter guns, which can host targets of 7.62 cm (3 inches) in diameter, are tilted at 3° and located 10 cm off-axis of the substrate.

The AZO thin films were deposited at room temperature onto 5×5 cm² 1737F Corning glass substrates by DC magnetron sputtering from a 99.99% purity ZnO:Al₂O₃ ceramic target composed of 98wt% ZnO and 2wt% Al₂O₃, which was purchased from Neyco. Before each deposition process, the glass substrate to be used was washed with deionized water and liquid soap, and then rinsed first with abundant water and second with abundant isopropanol. Finally, it was dried with nitrogen gas and placed on the holder-plate inside the sputtering chamber.

The distance from the center of the target to the center of the substrate was fixed at 18 cm and a substrate rotation of 13 rpm was used to achieve good homogeneity. The films were deposited with a DC power of 120 W [which corresponds, when divided by the target area (45.60 cm²), to a power density of 2.63 W/cm²] and under a deposition

pressure equal to 4.0 mTorr (0.53 Pa), which was maintained solely with argon gas (99.99% purity) by employing a constant argon flow rate of 20 sccm.

The effect of the base pressure was studied in the interval from 1.1×10^{-5} Torr ($\sim 1.5 \times 10^{-3}$ Pa) to 4.0×10^{-7} Torr ($\sim 5.3 \times 10^{-5}$ Pa). The vacuum was achieved using a dry primary pump and a high-vacuum turbomolecular pump (500 L/s), and it should be taken into account that no load lock chamber was used. The different base pressure values, which were measured with a Granville-Phillips 274 Bayard-Alpert type ionization vacuum gauge, were obtained by varying the pumping time before deposition. Thus, as shown in Figure 1, a longer pumping time achieved a lower base pressure (that is, higher vacuum level).

Furthermore, because the dependence of the base pressure (especially the water vapor content) with pumping time can be affected by the time the sputtering chamber was maintained open and by the ambient humidity, and likely by how long the cleaned substrates were exposed to the ambient (and here the humidity again) before being placed in the holder-plate inside the sputtering chamber, these variables were attempted to be held under control, and especially the times for each process. By following this method, we tested 25 base pressure values chosen randomly within the range and without following a sequential increase or decrease of base pressure.

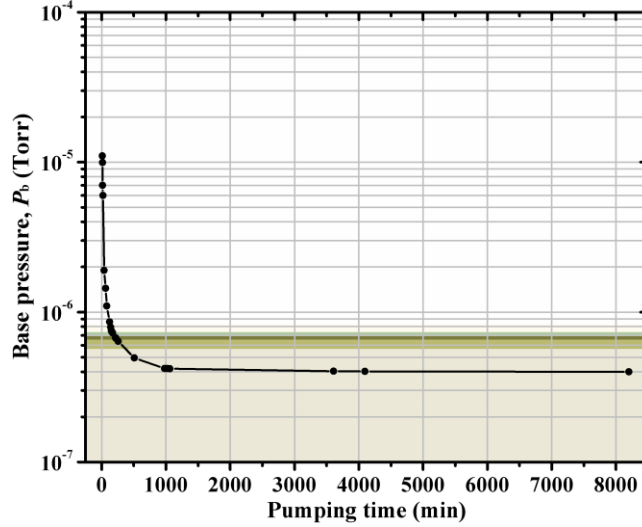


FIG. 1. (Color online) Relation between the base pressure achieved in the sputtering chamber and the pumping time for the 25 different samples studied in the present work.

Although there was some difficulty arising from a variation of deposition rate (especially in a narrow range of base pressure, which will be discussed in the following sections), we intended to control the deposition time to achieving AZO thin films with a thickness of 200 nm. These films were fully characterized and the films thinner or thicker than 200 ± 20 nm were only characterized for the electrical and chemical properties with the assumption that these properties do not largely depend on thickness.

B. Characterization techniques

The thickness of all of the deposited AZO thin films was measured with a Dektak 3030 profilometer, for which a simple lift-off technique was used on the films. The sheet resistance of the AZO thin films was measured with a Jandel RM3 four-point probe system, and the resistivity was calculated by multiplying the measured thickness and the sheet resistance.

For the optical properties, the percent transmittance ($\%T$) was recorded with a PerkinElmer Lambda 950 UV/Vis/NIR spectrometer using air as the reference, where the measurements were obtained with the AZO film facing the incident light. The measured $\%T$ was integrated in the interval of 400 to 1100 nm.

For the analysis of the chemical composition of the material, the AZO thin films were measured by X-ray photoelectron spectroscopy (XPS) by using a PHI Multitechnique system (from Physical Electronics) with a monochromatic X-ray source from the Al $K\alpha$ line possessing an energy of 1,486.8 eV. The measurements were obtained after an erosion treatment with an argon ion sputtering performed in the XPS system, and, due to the difficulty to identify the Ar $2p_{3/2}$ peak (which must be located at about 241.83 eV), the binding energies of the recorded spectra were charge-corrected by referencing the center of the whole Ar $2p$ signal to 242.05 eV, according to our previous observation on argon implanted in sputtering-deposited Al_2O_3 .³⁷

The structure of the deposited material was analyzed by means of a PANalytical X'Pert PRO MPD Alpha 1 powder X-ray diffractometer. The crystallite size was calculated from the X-ray diffraction (XRD) patterns by using the Scherrer equation:³⁸⁻⁴⁰

$$D = \frac{K\lambda}{B_{2\theta} \cos \theta}, \quad (1)$$

where D represents the mean dimension of the crystallite perpendicular to the diffraction plane; K is the shape factor, for which we employed the typical value of 0.9; λ is the wavelength of the X-ray used in the diffractometer, whose value is 0.15406 nm; $B_{2\theta}$ is the full width at half maximum (FWHM) of the diffraction line in radians; and θ is the diffraction angle for the diffraction line position, for which the diffraction peak with the highest intensity was selected.

III. RESULTS AND DISCUSSION

A. Color

The first and most evident result of the experiments was the color of the deposited AZO thin films, which are shown in Figure 2. Using the colors observed in Figure 2, we divided the base pressure axis in Figure 1 and almost all the subsequent figures into color zones according to the approximate appearance of the corresponding produced film (we used the physical appearance when watching the light through the films). Here, we observed that all of the AZO thin films deposited at a high base pressure were very transparent to the eye (transparent zone). However, there exists a point of good vacuum ($\sim 7.3 \times 10^{-7}$ Torr) in which the films appeared as dark grayish, which became darker (with a brownish appearance) as the vacuum level was improved (opaque zone). Finally, the thin films were moderately transparent, exhibiting a dark yellowish color, at the lowest base pressure values (under $\sim 5.7 \times 10^{-7}$ Torr: dark yellow zone).

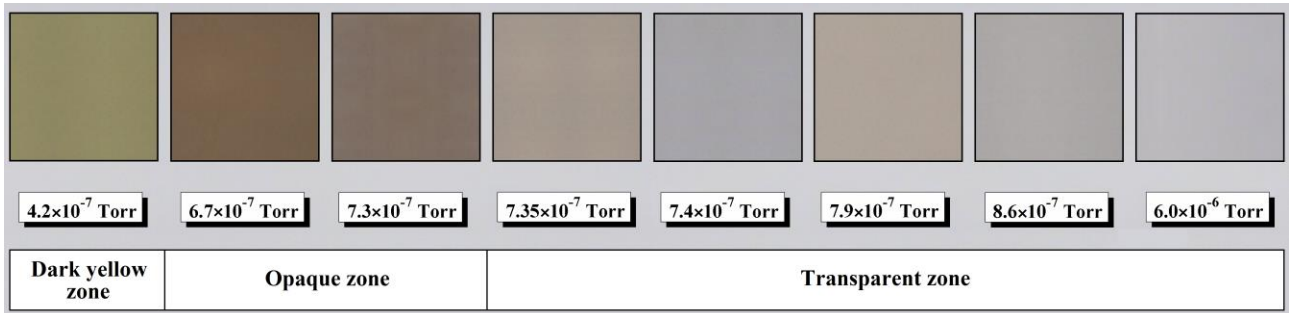


FIG. 2. (Color online) Digital photographs of the AZO thin films deposited at the most representative base pressure values, from 4.2×10^{-7} Torr (left) to 6.0×10^{-6} Torr (right).

The AZO thin films were placed on a white paper sheet, which is the background color of the figure. Although the background looks gray to the eye owing to the digitalization of

the figure, it constitutes a reference for comparison: the AZO films deposited at higher base pressure (right) show a color similar to the background, indicating its high transparency.

The observation of the color of the films was the first convincing indication of the great dependence of the AZO properties with the base pressure, which, as observed in Figure 3, do not show a simple tendency. In this figure, we present in pairs the main parameters measured or calculated for the deposited AZO thin films. For reference, at the top of the graphs, in Figure 3(a), the thickness of the films is plotted, and the different regions of base pressure are tinted according to the color of the resulted films. These regions (zones) are formally represented by the integrated $\%T$ [Figure 3(d)], which is discussed in following subsections.

Because Figure 3 contains all of the results of the present work, the following points are very important for a better discussion of each experimental observation:

- a) The base pressure values were taken from the corresponding pumping time according to Figure 1, which was the real experimental variable used in this work. Although the base pressure values are not exact, in this paper they will be considered as real and strict values. For example, the values inserted at the top of Figure 3 [7.3×10^{-7} Torr ($\sim 9.7 \times 10^{-5}$ Pa) and 5.7×10^{-7} Torr ($\sim 7.6 \times 10^{-5}$ Pa)] are rigidly considered in this paper as real vacuum zone borders. However, the reader is asked to remember the flexibility of such values and the difficulty to measure the base pressure values with accuracy.

- b) We tested 25 base pressure values. Among them, 10 values are in or near the narrow opaque zone. Because all of the base pressure values are studied randomly, without following a sequential increase or decrease of base pressure, the observed abrupt change of the measured or calculated parameters in the opaque zone is a real observation.
- c) The measured or calculated values for the different parameters studied were connected with a solid line in the plots of Figure 3 only with the aim of guiding the eye.

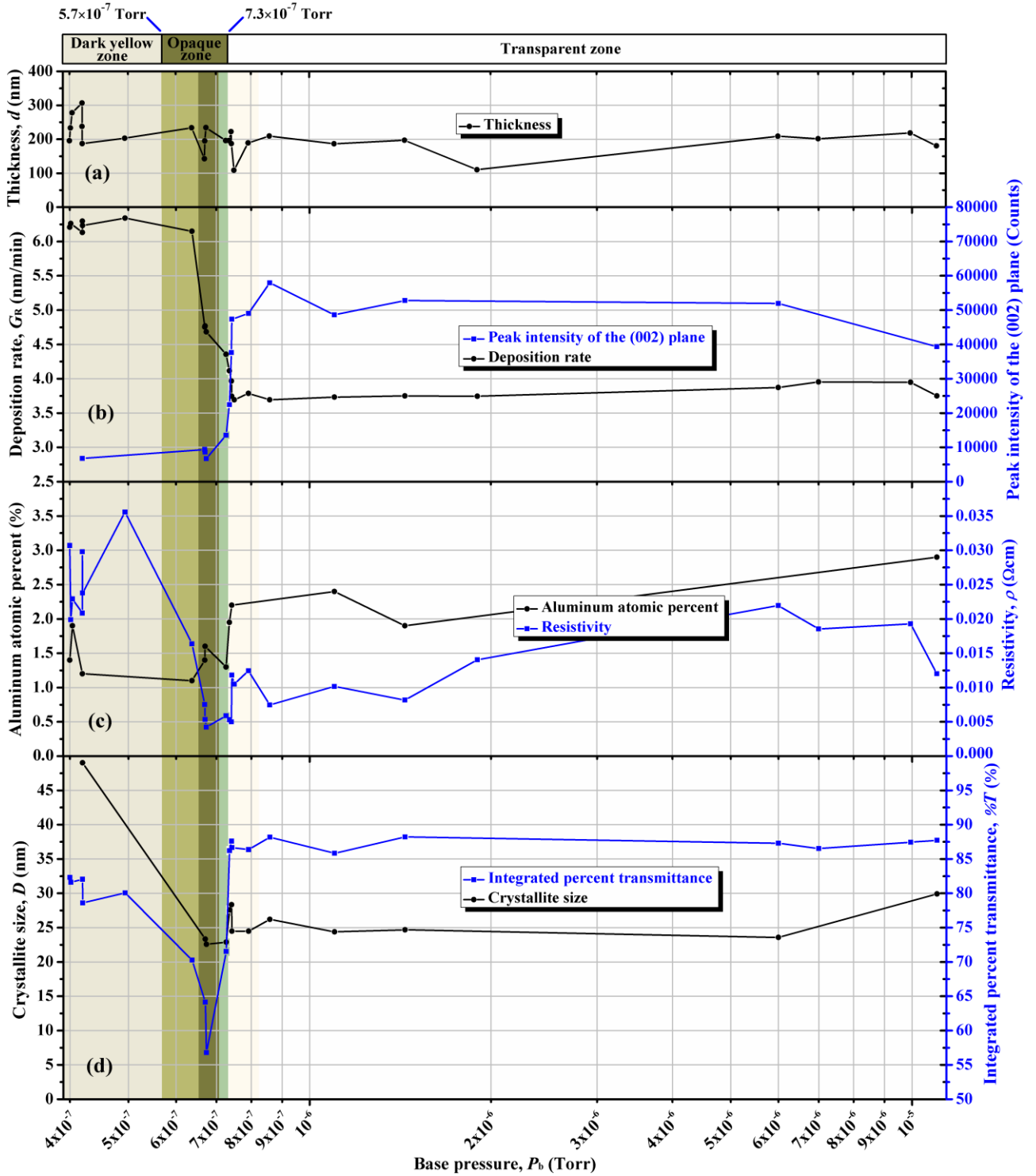


FIG. 3. (Color online) Variation of the (a) thickness, (b) intensity of the (002) plane peak and deposition rate, (c) aluminum atomic percent content and resistivity, and (d)

integrated percent transmittance and crystallite size of the AZO thin films as a function of the base pressure achieved before the sputtering deposition.

B. Deposition rate and structure

The first parameter measured was the thickness of the samples [Figure 3(a)]. From the thickness and the deposition time, which was not the same for all samples, we calculated the deposition rate by assuming that it was constant during the film growth. In Figure 3(b) it should be noted that the thin films deposited in the highest base pressure zone (from $\sim 1.1 \times 10^{-5}$ to $\sim 7.4 \times 10^{-7}$ Torr: transparent zone), which produces transparent AZO thin films, grow with a low deposition rate, which is almost constant with values between 3.7 and 4.0 nm/min. We observe that the lowest base pressure value identified within this transparent zone, $\sim 7.4 \times 10^{-7}$ Torr, constitutes a real vacuum border, since simply by lowering the base pressure to $\sim 7.3 \times 10^{-7}$ Torr the AZO thin film grow with a deposition rate of 4.4 nm/min and appear greyish. Notably, before this last value we identify a base pressure point to which we assign the intermediate value of 7.35×10^{-7} Torr, which produces a deposition rate of 4.1 nm/min and belongs to the transparent zone. This further delimits the transparent-opaque border. By further lowering the base pressure, the deposition rate exhibits a sharp increase along the narrow opaque zone of base pressure (from $\sim 7.3 \times 10^{-7}$ to $\sim 5.7 \times 10^{-7}$ Torr) until it reaches the value of 6.2 nm/min. This value is maintained at almost a constant level in all the lowest base pressure zone (from $\sim 5.7 \times 10^{-7}$ to $\sim 4.0 \times 10^{-7}$ Torr: dark yellow zone), although the AZO thin films produced appear dark yellowish, but more transparent.

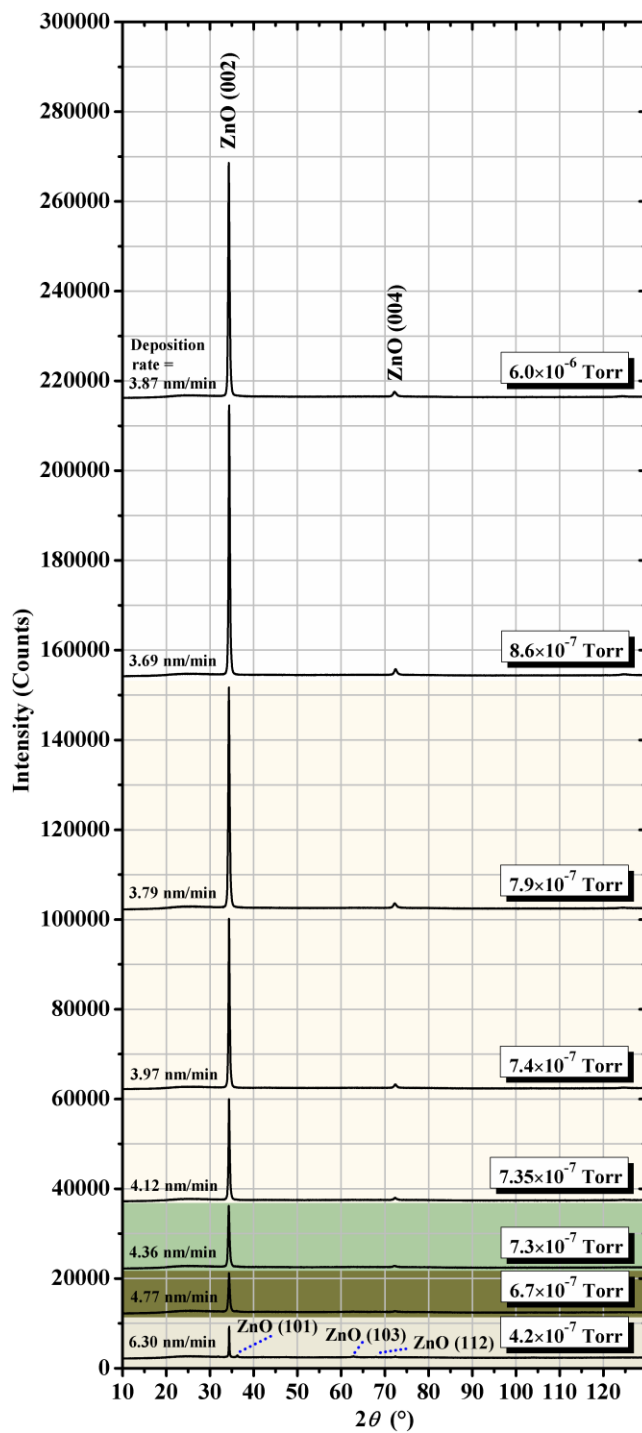


FIG. 4. (Color online) X-ray diffractograms of the 200 ± 20 -nm AZO thin films deposited at the most representative base pressure values. See Figure 5 to see more detail of the low-intensity peaks.

Figure 4 shows the XRD patterns of the AZO thin films deposited at the most representative base pressure values. All of the recorded diffractograms exhibit an intense peak around 34.3° , which corresponds to the (002) crystalline plane of the ZnO hexagonal wurtzite structure. This indicates a *c*-axis preferred orientation perpendicular to the substrate surface. A second low-intensity peak is observed around 72.3° , which corresponds to the (004) plane of the same hexagonal structure. It is clearly observed from the (002) plane peak intensity that at higher base pressure (that is, at a bad vacuum level) the AZO thin films exhibit a better degree of crystallinity. Also, it is observed that the (002) peak intensity exhibits a strong inverse dependence on deposition rate, which is clearly observed in Figure 3(b). In the transparent zone, where the AZO thin films grow with a slow deposition rate, the (002) plane peak exhibits the highest intensity. As the base pressure reaches the transparent-opaque border, the deposition rate slightly increases and the intensity of the (002) plane peak significantly decreases.

As seen in Figure 3(b), the most interesting base pressure values, from the higher to lower ones, begin with the point at the transparent-opaque border (7.35×10^{-7} Torr, mentioned previously), in which the deposition rate is 0.2 nm/min faster and the (002) plane peak intensity is reduced by 40% compared with the previously tested base pressure point (7.4×10^{-7} Torr, with a difference of only $\sim 0.5 \times 10^{-8}$ Torr). The next measured value is 7.3×10^{-7} Torr, being the first measured point of the opaque zone, producing a film with a dark grayish appearance. Here, again, the deposition rate is 0.2 nm/min faster and the (002) peak intensity is reduced again by 40% compared with the previous measured point (7.35×10^{-7} Torr). However, at this base pressure value we begin to detect, although very slightly, the peak of the (101) crystalline plane of the ZnO

hexagonal structure. This peak is more appreciable in Figure 5, where it is plotted to more clearly show the low-intensity peaks of these samples.

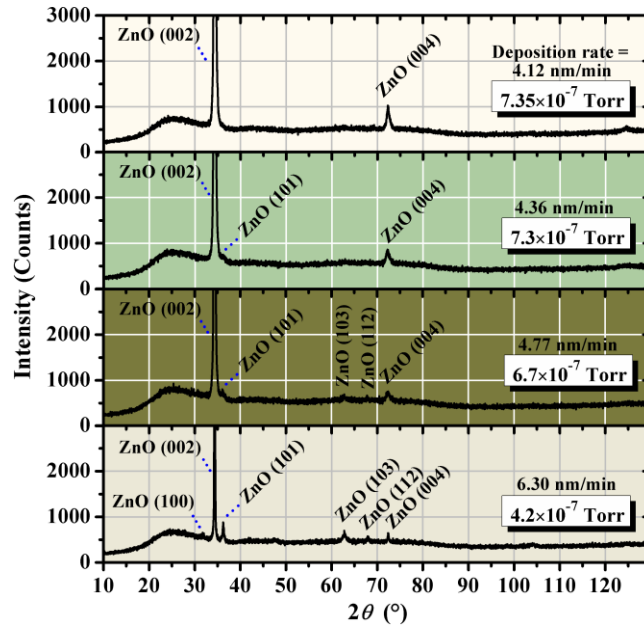


FIG. 5. (Color online) X-ray diffractograms of the 200 ± 20 -nm AZO thin films deposited at base pressure values near the transparent-opaque border, plotted in the y-axis up to 3,000 counts to more clearly show the low-intensity diffraction peaks.

It may be that the observed great progressive reduction in the crystalline fraction in the AZO material, denoted by the reduction of the peak intensity of the (002) plane and the rise of other diffraction peaks, is indirectly related with the darkening of the AZO films, which begins, in our case, with a dark grayish appearance. This reduction in crystallinity is accentuated with the slight appearance of other ZnO peaks corresponding to the (103) and (112) crystalline planes in the AZO film deposited at the next measured value (6.7×10^{-7} Torr), which also shows the lowest integrated %*T*. Similar results were observed by Chou & Liu on ZnO thin films,⁴¹ who attributed the dark appearance to the presence of some zinc excess. They observed that as some zinc excess is included in the

ZnO films, the XRD patterns change from a highly oriented (002) ZnO structure to a weakly crystallized and randomly oriented ZnO polycrystals. They also observed that when the intensity of the (002) peak of ZnO decreases due to the presence of excess of zinc, the (101) peak appears immediately. These observations coincide with our results; however, in our case, it was difficult to find a good correlation with the excess of zinc.

At this point, we partially conclude that the intensity of the peak corresponding to the (002) crystalline plane inversely depends on the deposition rate at which the AZO thin films grew. A low deposition rate leads to the formation of a low nuclei density resulting in a better crystallinity; while a high deposition rate culminates with the formation of a high density of defects, thereby reducing the crystalline fraction. The deposition rate of the AZO thin films, on the other hand, seems to depend on the base pressure. This last dependence on base pressure has been observed by Huo *et al.*,¹⁸ who explained the reduction of deposition rate of the AZO films as an effect of residual gases. They posited that the presence of residual gases in the argon plasma discharge causes more collisions and thus decreases the mean free path of the particles. An alternative explanation was given by Wang *et al.*²⁰ for the effect of the particular case of water vapor on the deposition rate of ITO films. They suggested that the deposition rate decreased in the presence of water vapor because the dissociation of the water molecules exhausted the electron energy in the plasma, which resulted in the suppressed ionization of argon and, hence, in an affected deposition rate.

C. Electrical properties and chemical composition

In Figure 3(c) we plot the resistivity and the aluminum content, expressed as atomic percent, of the AZO thin films as a function of the base pressure. The variation of

resistivity with base pressure is one of the most interesting results of this study because we observe a tendency similar to the U-shaped behavior observed by Zebaze-Kana *et al.* on ITO films,¹⁵ but in a more extensive range (plotted in logarithmic scale) of base pressure. The best consensus on the explanation of this U-shaped behavior was given by researchers who studied the effect of the addition of H₂ gas during the deposition of the films. Because the resistivity (ρ) is proportional to the reciprocal of the product of the carrier concentration (n) and the carrier mobility (μ), according to

$$\rho = \frac{1}{ne\mu}, \quad (2)$$

(where e is the elementary charge) the expected resistivity must mainly depend on the carrier concentration naturally given by the known components of the material, such as concentration of the intentionally added dopant, and on the mobility obtained with the structure and the crystallinity resulting from the usual sputtering deposition conditions (all of which are given by the optimized conditions of each research group). However, based on the calculations by Van de Walle,^{42,43} that were also confirmed by Cox *et al.*⁴⁴ and Hofmann *et al.*,⁴⁵ some authors suggested that the addition of H₂ gas in the sputtering chamber incorporates hydrogen atoms into the deposited material (both ITO and AZO), which acts as a shallow donor. This results in an increase of carrier concentration and, according to Eq. (2), in the reduction of resistivity.^{31,33,35} Also, because hydrogen is a strong reducing species, it affects the incorporation of oxygen into the deposited film, which produces oxygen vacancies and thereby further reduces the resistivity.^{21–28,31,33,35,36} This is the lowest point in the observed U-shaped behavior. Then, a further increase of H₂ gas over-saturates the H-doping stage and/or generates a large density of oxygen vacancies. This produces a reduction of crystallinity and mobility, which is translated into

an increase of resistivity and, owing to the oxygen deficiency, into a decrease of transmittance. This is the right-hand side of the U-shaped behavior of resistivity.

Because we observed neither a decrease of transmittance nor a decrease of crystallinity in the AZO thin films with the increase of the base pressure (the same was observed by Zebaze-Kana *et al.*¹⁵ when they studied the effect of the base pressure on ITO), the previous explanation seems to be partially operating in our case. Here, it is important to mention that the main residual gas in the sputtering chamber is water vapor,^{3,14} which also produces oxygen atoms after dissociation. Therefore, there may be other factors also participating in the mechanism behind the observed results. The only systematic information regarding the effect of water vapor was given by Eisgruber *et al.*¹⁹ and Wang *et al.*,²⁰ and it is related to ITO. Although they did not fully explain their results, they observed the same U-shaped tendency when studying the effect of water vapor on the resistivity of ITO films. However, Eisgruber *et al.*¹⁹ also pointed out that the addition of water vapor improves both the resistivity (by following the U-shaped behavior) and transmittance, as well as leading to a progression in the crystalline structure. Furthermore, they highlighted that the addition of water is not equivalent to the addition of O₂ gas into the sputtering chamber, since oxygen, although improving transmittance, always increases the resistivity of ITO. Therefore, a good explanation of these results must include the effect of both hydrogen and oxygen atoms. So, it may be that while hydrogen reduces resistivity by acting as a shallow donor on the one hand, oxygen atoms incorporate into the deposited film (confirmed by Wang *et al.*²⁰) and compensate for the reducing effect of hydrogen, on the other hand. This avoids the further lack of oxygen discussed in the previous paragraph, and thus avoids both the loss

of crystallinity and the worsening of transmittance. This better fits, to a certain extent, with our observations.

Regarding to Figure 3(c), there is another important factor that should not be missed: the base pressure affects the aluminum content of the deposited AZO thin films. This ranges from 1.1 to 2.9% without following an obvious tendency. The variation of aluminum content was also observed in AZO films by Addonizio *et al.*³⁰ and Liu *et al.*,³¹ but as a function of the addition of H₂ in the sputtering chamber. They observed aluminum content variations of 2.0–2.8% and 1.9–2.2%, respectively. Because the Van de Walle theory^{42,43} was not yet developed when Addonizio *et al.*³⁰ reported their observations, they related the electrical changes owing to the H₂ addition with the effectiveness of the aluminum doping in terms of the atom position in the lattice. Liu *et al.*,³¹ who observed a negligible variation of aluminum content, opted for the Van de Walle theory and the formation of oxygen vacancies, where the latter may be owing to the reducing effect of hydrogen.

Because we observed a large variation in aluminum content with the change of base pressure, the explanation of the resistivity behavior becomes enormously complicated. Any explanation of the resistivity behavior with base pressure, according to Eq. (2), must include the variation of carrier concentration owing to aluminum doping, hydrogen doping, and oxygen vacancies on the one hand, and the variation of mobility owing to crystallinity and crystallite size on the other hand. For example, the observed relation between resistivity and aluminum content is maintained only in short sections of base pressure range (discussed below), but not along the entire base pressure interval studied, which indicates the importance of the other parameters. Because all of the

parameters were affected by the base pressure, as observed in Figure 3, it is very difficult to give a full explanation of the U-shaped behavior of resistivity.

In this paragraph, we mainly consider the effect of aluminum content, for which it is convenient to begin from the lowest base pressure studied; that is, where the effect of residual gases is minimal. Here, the reader is referred to Figure 6 to clarify the relation between resistivity and aluminum content for only those samples presenting a thickness of 200 ± 20 nm, which were fully characterized with all of the techniques (indicated in the Experimental section). First, the worst resistivity values were exhibited by those thin films deposited after the lowest base pressure was achieved (dark yellow zone), which can be related (at least) to the low crystalline fraction of the AZO films [Figure 3(b)] and the low content of aluminum. Interestingly, one AZO thin film among the group possessed an aluminum content of 1.9% (4.05×10^{-7} Torr) and exhibited the lowest resistivity, which indicates that, although this value deviates from the series, in this base pressure section the relation between both parameters exists (an aluminum content of 2% is assumed as optimum). By increasing the base pressure until the opaque zone is reached, the AZO thin films exhibit an improved conductivity. In this region (the upper and lower red boxes in Figure 6), where the films still exhibit low crystallinity, the content of aluminum is between 1.3% (7.3×10^{-7} Torr) and 1.6% (6.7×10^{-7} Torr), where the film with 1.6% aluminum content (6.7×10^{-7} Torr) exhibits the better conductivity. Since these films are electrically superior to the thin film mentioned with 1.9% aluminum content (4.05×10^{-7} Torr) deposited with minimal residual gases, we suggest that the small increase in crystallinity and doping with residual gases (possibly mainly with hydrogen atoms) take importance. The next interesting base pressure point corresponds to the

transparent–opaque border (7.35×10^{-7} Torr, also enclosed in the red boxes in Figure 6), where the crystallinity significantly rises and the content of aluminum is almost 2.0%; here, the resistivity is the lowest among the samples studied. In the next base pressure point (7.4×10^{-7} Torr) the resistivity increases, possibly owing to an excess in aluminum content (although slight), which was determined to be 2.2%. For the following points, when the aluminum content exceeds 2% the resistivity is moderately high, but always better than the resistivity of the AZO thin films deposited with the lowest content of residual gases.

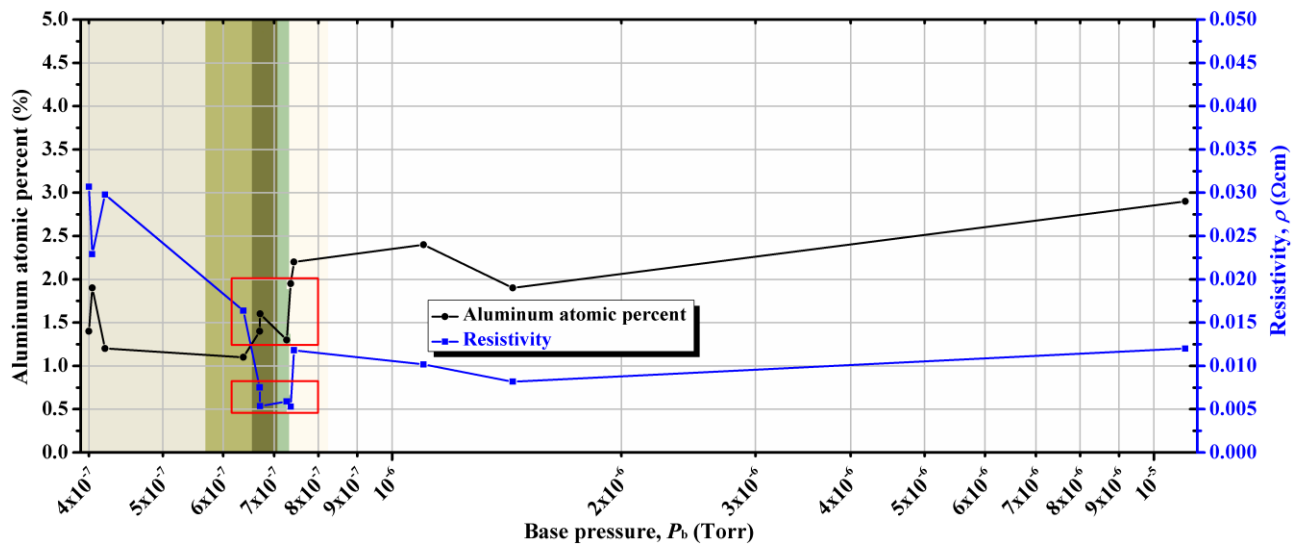


FIG. 6. (Color online) Relation between aluminum content and resistivity of the 200 ± 20 -nm AZO thin films expressed as a function of base pressure.

A definitive explanation of the observed resistivity behavior is a difficult task. However, the observed results are very interesting for selecting those ranges of base pressure that lead to better electrical properties, and even better transmittance. There are three obvious base pressure zones which each result in a similar resistivity, and also

nearly coincide with the physical appearance of the films (the color zones). The first zone (dark yellow zone), characterized by the good vacuum levels, always results in dark yellowish films with the worst conductivity. The use of mid-vacuum levels, in the second zone (opaque zone), results in dark AZO thin films with an improvement of the electrical properties as the transparent–opaque border is reached. A very low resistivity is obtained in the transparent–opaque border, which results in a transparent AZO thin film. However, this border is extremely narrow, and it is very difficult to maintain this vacuum level because a small change in the pumping time leads to a dark and good-conducting film on the one hand, or a moderately-conducting and transparent film on the other hand, depending on the direction of this deviation from the narrow border. The third zone (transparent zone) results in transparent AZO thin films with moderate resistivity. The vacuum levels of this transparent zone are easily achieved with short pumping times, which is an advantage. Therefore, for depositing TCOs we suggest the use of vacuum values lying in the transparent zone, and especially near the transparent–opaque border.

D. Crystallite size and optical properties

In Figure 3(d) we plotted the crystallite size and the integrated %*T* of the AZO thin films with a thickness of 200 ± 20 nm (the reader is referred to Figure 7 to observing the %*T* spectra of the 200 ± 20 -nm AZO films deposited at the most representative base pressure values). It is observed from Figure 3(d) that the values of the crystallite size are almost constant for each color zone, and that any slight variations in each zone are better related with the thin film thickness, which was not exactly 200 nm. Also, we observed a small correlation of the crystallite size with the resulted integrated %*T*, which, as discussed in previous subsections, seems to be mainly correlated with the peak intensity

of the (002) plane and the appearance of other crystalline planes. We observed that at lower base pressures (the opaque zone) the AZO thin films produced were darker, which coincided with the observed lower crystallinity. However, at the lowest base pressure zone (dark yellow zone) the integrated %*T* rises to moderate values while the crystallinity worsens. This means that maybe both %*T* and crystallinity are products of one determinant factor not yet well identified in this work. However, the small dependence observed between crystallite size and the integrated %*T* probably constitute another influential factor, because although the dark yellowish films deposited with the lowest content of residual gases exhibit the lowest crystalline fraction, as indicated by the lowest peak intensity of the (002) crystalline plane, they also present the biggest crystallite size.

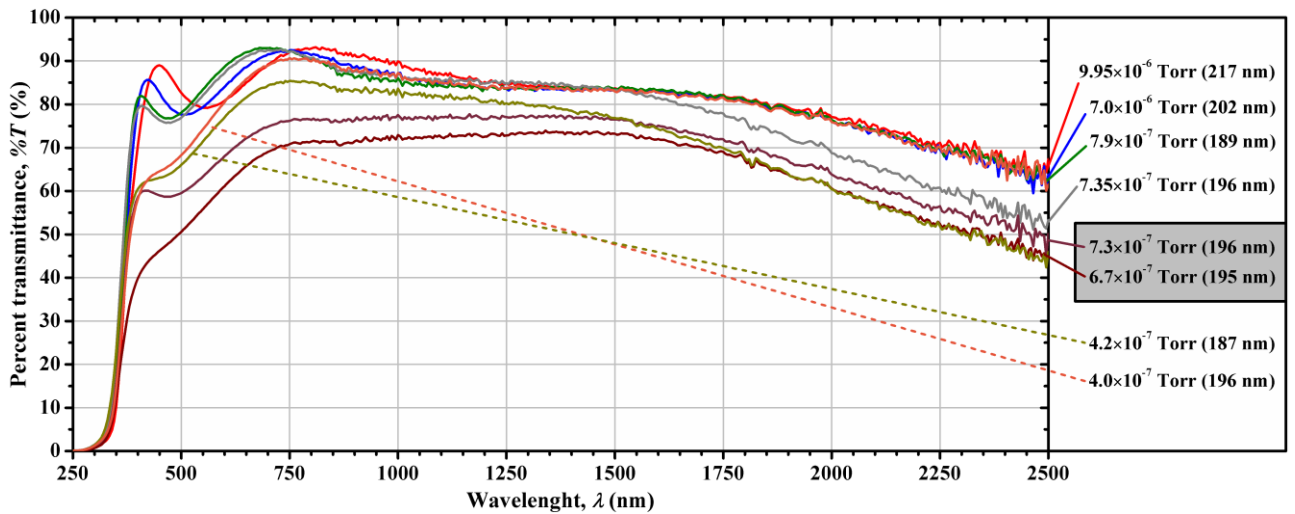


FIG. 7. (Color online) Percent transmittance spectra of 200±20-nm AZO thin films deposited after achieving different base pressure values.

We also attempted to correlate the optical properties with the chemical composition (for example, an excess of zinc content), but the distribution of zinc and oxygen as a function of base pressure did not exhibit any obvious tendency. Therefore, in

the present study we do not explain the real mechanism defining the absorption in the visible range as a function of base pressure. However, to find a good correlation a careful chemical analysis is required, and this will be better addressed in a subsequent paper (as a general comparison, Figure 8 shows the survey spectra of three AZO samples representative of each base pressure zone).

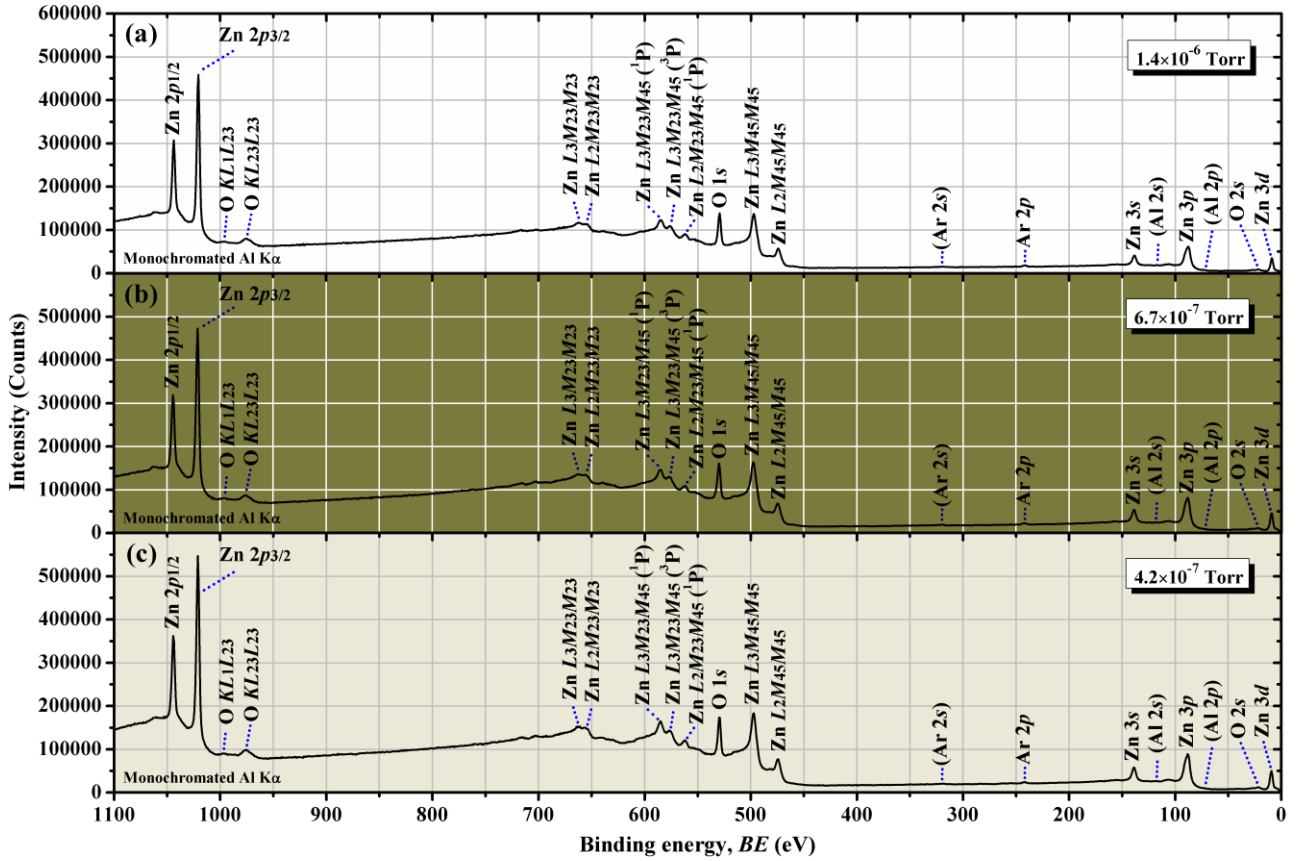


FIG. 8. (Color online) Survey X-ray photoelectron spectra of three AZO thin films taken as examples for the (a) transparent zone, (b) opaque zone, and (c) dark yellow zone.

E. Stability to the environment

In the body of this paper we mentioned that the best zone in which to work without technical difficulties is the transparent zone, which gives properties that are

almost constant within the zone. Furthermore, the pumping time in this zone is short. The transparent–opaque border is even better, but the control of this base pressure value is very difficult. However, we conducted another experiment to assist further in the selection of the optimum base pressure in which to work: the stability of the deposited AZO thin films to the environment. For this, we again measured the resistivity of the thin films after one month of aging in the ambient air (under uncontrolled humidity and light). The resistivity of the films measured one day and one month after their deposition are plotted in Figure 9. Here, we can observe that the AZO thin films deposited at the lowest base pressure zone are the most unstable to the environment. The films exhibiting superior stability are those deposited around the transparent–opaque border, with a wide margin to the transparent zone (red box in Figure 9). We conclude therefore that the best vacuum zone in which to deposit TCOs is the transparent zone, and especially near to the transparent–opaque border, and particularly in the range from 7.35×10^{-7} to 1.5×10^{-6} Torr. One of the objectives of the present study is to demonstrate to other research groups the importance of the base pressure achieved prior the material deposition, and to motivate them to identify the base pressure range that produces TCOs with the best and most reproducible characteristics and properties for their particular systems.

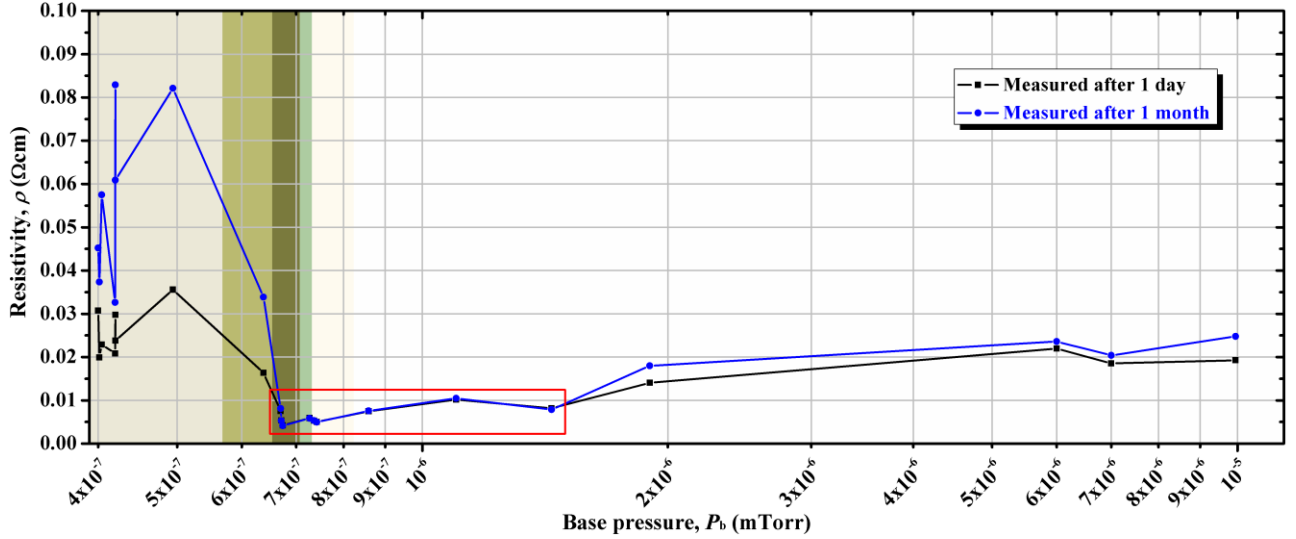


FIG. 9. (Color online) Change of resistivity of the AZO thin films measured one day and one month after the deposition, expressed as a function of base pressure.

IV. CONCLUSIONS

We deposited 200 ± 20 -nm AZO thin films by magnetron sputtering using a DC power of 120 W and a deposition pressure equal to 4.0 mTorr (0.53 Pa) with only argon gas, after achieving different base pressure values. We tested a random distribution and order of 25 points of base pressure in the interval from 1.1×10^{-5} Torr (1.5×10^{-3} Pa) to 4.0×10^{-7} Torr (5.3×10^{-5} Pa), and we observed a strong influence of this real deposition parameter on the deposition rate, peak intensity of the (002) crystalline plane, resistivity, aluminum content, crystallite size, and transmittance of the deposited AZO thin films, though no simple tendency was observed.

The first indication of the effect of the base pressure was the color of the deposited AZO thin films. Based on this, we divided the studied interval of base pressure into three zones, that each produced thin films exhibiting similar properties and

characteristics. These zones were labeled the dark yellow zone, opaque zone, and transparent zone. The dark yellow zone [good vacuum level: 4.0×10^{-7} Torr (5.3×10^{-5} Pa) to 5.7×10^{-7} Torr (7.6×10^{-5} Pa)] produced dark yellowish AZO thin films with a moderate transmittance (%*T* of 78.6–82.3%) and presenting the lowest crystalline fraction (but the largest crystallite size), the highest resistivity ($20\text{--}36 \times 10^{-3}$ Ωcm), and the worst stability to the environment. The opaque zone [mid vacuum level: 5.7×10^{-7} Torr (7.6×10^{-5} Pa) to 7.3×10^{-7} Torr (9.7×10^{-5} Pa)] produced dark AZO thin films (with %*T* up to 56.8%) with low crystallinity and good conductivity (resistivity up to 4×10^{-3} Ωcm). The transparent zone [bad vacuum level: 7.35×10^{-7} Torr (9.80×10^{-5} Pa) to 1.1×10^{-5} Torr (1.5×10^{-3} Pa)] produced AZO thin films with the highest transmittance (with %*T* of 85.8–88.2%), the highest crystalline fraction, and presenting moderate resistivity (between 5×10^{-3} and 20×10^{-3} Ωcm).

We observed that the best AZO thin film was deposited at the border between the opaque and transparent zone [7.35×10^{-7} Torr (9.80×10^{-5} Pa), in the transparent zone], presenting a resistivity of 5×10^{-3} Ωcm and an integrated %*T* of 87%. However, this base pressure value was very difficult to obtain because a small change in the pumping time produced a dark and good-conducting film (in the opaque zone) on the one hand, or a transparent but moderately-conducting film (in the transparent zone) on the other hand, depending on the deviation from this narrow border. We found, however, that the values around this narrow border and especially in the direction of higher base pressure up to 1.5×10^{-6} Torr (2.0×10^{-4} Pa), produce highly transparent AZO thin films with adequate resistivity and high stability to the environment. Therefore, the optimum base pressure

range at which to deposit AZO thin films is from 7.35×10^{-7} Torr (9.80×10^{-5} Pa) to 1.5×10^{-6} Torr (2.0×10^{-4} Pa).

We also observed that the intensity of the peak corresponding to the (002) crystalline plane inversely depends on deposition rate, where the rate increases as the achieved base pressure is lower (that is, when the vacuum level is higher). Therefore, the residual gases at a high base pressure, whose presence probably affects the energy of the particles in the plasma, work to reduce the deposition rate and thereby lead to an increase of the (002) plane peak. A low base pressure, on the contrary, leads to a low-crystallinity material, an observation that coincides with the darkening of the films. Furthermore, we observed an increase of transmittance (with a dark yellowish color) of the films deposited in the lowest base pressure zone, which also coincides with the increase of the crystallite size. Maybe both crystallinity and transmittance in the visible range depend on another factor not identified in the present work.

On the other hand, the dependence of resistivity with the base pressure followed a tendency similar to the U-shaped behavior observed by other authors but mainly as an effect of the addition of water vapor and H_2 gas into the sputtering chamber. The tendency observed in this work when the base pressure is varied is the total result of the change of hydrogen content (not determined), aluminum content (1.1–2.9%), oxygen vacancies (not determined), interstitial zinc (not determined), crystallinity, crystallite size, and possibly other parameters.

ACKNOWLEDGMENTS

The *Centres Científics i Tecnològics de la Universitat de Barcelona* (CCiTUB) are acknowledged for the assistance in XRD and XPS measurements. This work was

supported by the Spanish *Ministerio de Economía y Competitividad* (MINECO) through the project HELLO (ENE2013-48629-C4-2-R). Jorge Alberto García-Valenzuela gratefully acknowledges the financial support from the Mexican *Consejo Nacional de Ciencia y Tecnología* (CONACyT) with registration numbers 208159 and 251082.

¹M. J. Rocke, *J. Vac. Sci. Technol.*, A **6**, 1675 (1988).

²F. Yoshizaki and T. Kingetsu, *Thin Solid Films* **239**, 229 (1994).

³D. L. Windt, W. L. Brown, C. A. Volkert, and W. K. Waskiewicz, *J. Appl. Phys.* **78**, 2423 (1995).

⁴P. Lv, Z.-Q. Zhang, J.-T. Guan, X.-D. Wang, X.-L. Hou, L.-Y. Zhang, J.-J. Wang, B. Chen, and Q.-F. Guan, *Sci. China-Phys. Mech. Astron.* **56**, 1689 (2013).

⁵J. S. Chen, B. C. Lim, and T. J. Zhou, *J. Vac. Sci. Technol. A* **23**, 184 (2005).

⁶A. Asthana, Y. K. Takahashi, Y. Matsui, and K. Hono, *J. Magn. Magn. Mater.* **320**, 250 (2008).

⁷K. Takahashi, S. Masuda, Y. Tsukayama, A. Kadowaki, Y. Matsumara, and Y. Nishi, *J. Jpn. Inst. Met.* **69**, 671 (2005); Y. Nishi, Y. Matsumara, and K. Takahashi, *Mater. Trans.* **47**, 2852 (2006).

⁸M.-J. Jeng, W.-K. Lei, W.-L. Ku, L.-B. Chang, C.-W. Wu, Y.-T. Lu, and S.-C. Hu, *Adv. Mater. Res.* **213**, 161 (2011).

⁹G. S. Frankel, X.-B. Chen, R. K. Gupta, S. Kandasamy, and N. Birbilis, *J. Electrochem. Soc.* **161**, C195 (2014).

¹⁰J. Li, L. Hou, H. Ruan, Q. Xie, F. Gan, *Proc. SPIE* **4085**, 125 (2001), edited by F. Gan and L. Hou, presented at: Fifth International Symposium on Optical Storage (ISOS 2000), Shanghai, China, May 22–26, 2000.

- ¹¹H. Jiang, J. Zhu, Q. Huang, J. Xu, Q. Wang, Z. Wang, S. Pfauntsch, and A. Michette, *Appl. Surf. Sci.* **257**, 9946 (2011).
- ¹²M.-H. Chan and F.-H. Lu, *Surf. Coat. Technol.* **203**, 614 (2008).
- ¹³L.-R. Yao and F.-H. Lu, *Int. J. Appl. Ceram. Technol.* **10**, 51 (2013).
- ¹⁴B. H. Lee, C.-H. Yi, I. G. Kim, and S.-H. Lee, *MRS Proc.* **424**, 335 (1997), edited by F. Funada, M. K. Hatalis, J. Kanicki, and C. J. Summers, presented at: 1996 MRS Spring Meeting, San Francisco, California, USA, April 4–12, 1996; B. H. Lee, I. G. Kim, S. W. Cho, and S.-H. Lee, *Thin Solid Films* **302**, 25 (1997).
- ¹⁵M. G. Zebaze-Kana, E. Centurioni, D. Iencinella, and C. Summonte, *Thin Solid Films* **500**, 203 (2006).
- ¹⁶D.-K. Kim and H.-B. Kim, *J. Alloys Compd.* **522**, 69 (2012).
- ¹⁷N. Itagaki, K. Oshikawa, K. Matsushima, I. Suhariadi, D. Yamashita, H. Seo, K. Kamataki, G. Uchida, K. Koga, and M. Shiratani, presented at: 13th International Conference on Plasma Surface Engineering (PSE 2012), Garmisch-Partenkirchen, Germany, September 10–14, 2012, pp. 84–87.
- ¹⁸H.-Y. Huo, M. Zou, G.-Q. Ma, and H. Chang, *Surf. Technol. (China Acad. J.)* **42**, 75 (2013) (in Chinese).
- ¹⁹I. L. Eisgruber, J. R. Engel, R. E. Hollingsworth, P. K. Bhat, and R. Wendt, *J. Vac. Sci. Technol., A* **17**, 190 (1999).
- ²⁰M. H. Wang, Y. Onai, Y. Hoshi, H. Lei, T. Kondo, T. Uchida, S. Singkarat, T. Kamwanna, S. Dangtip, S. Aukkaravittayapun, T. Nishide, S. Tokiwa, and Y. Sawada, *Thin Solid Films* **516**, 5809 (2008).
- ²¹K. Zhang, F. Zhu, C. H. A. Huan, and A. T. S. Wee, *J. Appl. Phys.* **86**, 974 (1999).
- ²²K. Zhang, F. Zhu, C. H. A. Huan, A. T. S. Wee, *Thin Solid Films* **376**, 255 (2000).
- ²³S. N. Luo, A. Kono, N. Nouchi, and F. Shoji, *J. Appl. Phys.* **100**, 113701 (2006).

- ²⁴D.-G. Kim, S. Lee, G.-H. Lee, and S.-C. Kwon, *Thin Solid Films* **515**, 6949 (2007).
- ²⁵S. Luo, K. Okada, S. Kohiki, F. Tsutsui, H. Shimooka, and F. Shoji, *Mater. Lett.* **63**, 641 (2009).
- ²⁶Y.-L. Lee and K.-M. Lee, *Trans. Electr. Electron. Mater.* **10**, 203 (2009); H. K. Jeoung and K. M. Lee, *Mater. Technol.* **29**, A34 (2014).
- ²⁷S. Luo, S. Kohiki, K. Okada, F. Shoji, and T. Shishido, *Phys. Status Solidi A* **207**, 386 (2010).
- ²⁸S. Luo, S. Kohiki, K. Okada, A. Kohno, T. Tajiri, M. Arai, S. Ishii, D. Sekiba, M. Mitome, and F. Shoji, *Appl. Mater. Interfaces* **2**, 663 (2010).
- ²⁹K. Okada, S. Kohiki, S. Luo, D. Sekiba, S. Ishii, M. Mitome, A. Kohno, T. Tajiri, and F. Shoji, *Thin Solid Films* **519**, 3557 (2011).
- ³⁰M. L. Addonizio, A. Antonaia, G. Cantele, and C. Privato, *Thin Solid Films* **349**, 93 (1999).
- ³¹W. Liu, G. Du, Y. Sun, Y. Xu, T. Yang, X. Wang, Y. Chang, and F. Qiu, *Thin Solid Films* **515**, 3057 (2007).
- ³²S. H. Lee, T. S. Lee, K. S. Lee, B. Cheong, Y. D. Kim, and W. M. Kim, *J. Phys. D: Appl. Phys.* **41**, 095303 (2008).
- ³³M.-C. Li, C.-C. Kuo, S.-H. Peng, S.-H. Chen, and C.-C. Lee, *Appl. Opt.* **50**, C197 (2011).
- ³⁴V. Klykov, I. Strazdina, and V. Kozlov, *Surf. Coat. Technol.* **211**, 180 (2012).
- ³⁵C.-C. Huang, F.-H. Wang, and C.-F. Yang, *Appl. Phys. A* **112**, 877 (2013).
- ³⁶C. G. Kuo, C. L. Li, C. C. Huang, F. H. Wang, C. F. Yang, and I. C. Chen, *Adv. Mater. Res.* **813**, 447 (2013); F.-H. Wang, C.-F. Yang, J.-C. Liou, and I.-C. Chen, *J. Nanomater.* **2014**, 857614 (2014).
- ³⁷J. A. García-Valenzuela, R. Rivera, A. B Morales-Vilches, L. G. Gerling, A. Caballero, J. M. Asensi, C. Voz, J. Bertomeu, and J. Andreu, *Thin Solid Films* **619**, 288 (2016).
- ³⁸P. Scherrer, *Nachr. K. Ges. Wiss. Göttingen, Math. Phys. Kl.* **1918**, 98 (1918).

- ³⁹B. E. Warren, *X-Ray Diffraction* (Dover Publications, Inc., Mineola, New York, USA, 1990
[Republication of the work originally published by Addison-Wesley Pub. Co., 1969])
p. 253.
- ⁴⁰R. Saravanan and M. Prema Rani, *Metal and Alloy Bonding: An Experimental Analysis —
Charge Density in Metals and Alloys* (Springer-Verlag London Limited, London,
England, UK, 2012) p. 26.
- ⁴¹K.-S. Chou and G.-K. Liu, *Mater. Chem. Phys.* **37**, 156 (1994).
- ⁴²C. G. Van de Walle, *Phys. Rev. Lett.* **85**, 1012 (2000).
- ⁴³C. G. Van de Walle and J. Neugebauer, *Nature* **423**, 626 (2003).
- ⁴⁴S. F. J. Cox, E. A. Davis, S. P. Cottrell, P. J. C. King, J. S. Lord, J. M. Gil, H. V. Alberto,
R. C. Vilão, J. Piroto-Duarte, N. Ayres de Campos, A. Weidinger, R. L. Lichti, and S.
J. C. Irvine, *Phys. Rev. Lett.* **86**, 2601 (2001).
- ⁴⁵D. M. Hofmann, A. Hofstaetter, F. Leiter, H. Zhou, F. Henecker, and B. K. Meyer, *Phys.
Rev. Lett.* **88**, 045504 (2002).